

Vehicle Mass Lightening by Design of Light-weight Structured Substrates for Catalytic Converters

Manuel Presti, Lorenzo Pace, Wilfried Müller, Olaf Witte-Merl

Emitec GmbH

Copyright © 2011 SAE International

ABSTRACT

The clear objective of future powertrain development is strongly characterized by lowest emission impact and minimum overall system cost penalty to the customer. In the past decades emission impact has been primarily related to both optimization of combustion process and exhaust after-treatment system efficiency. Nowadays, weight reduction is one of the main objectives for vehicular applications, considering the related improvements both in fuel consumption (i.e. CO₂ production) and engine-out emissions. The state of the art of catalytic converter systems for automotive ZEV-oriented applications has yet to be introduced into mass production.

This paper investigates the successful application of metallic turbulent structures for catalytic converters along with innovative packaging considerations, such as structured outer mantle, which lead to significant weight reductions, exhaust backpressure minimization and improved overall emission conversion efficiency. Virtual engineering, such as FEA and CFD simulation, has been used to optimize the substrate (matrix and mantle) and successively a comprehensive test procedure has been carried out to validate the innovative substrate architecture.

INTRODUCTION

In an effort to minimize the impact of vehicular traffic on the environment and the people living in it, the regulatory authorities are passing more stringent legislation regulating the exhaust gas pollutants.

Additionally, increasing attention is drawn to vehicle mass reduction in order to decrease tailpipe CO₂ emission. One important approach to achieve this goal is to reduce the exhaust system weight. In particular, the present paper deals on one side with the mass reduction of the catalytic converter addressing both its internal architecture (substrate) and the outer shell (mantle).

On the other side, the present work addresses also the optimization of the conversion efficiency both in terms of light-off performance (related to converter's thermal mass) as well as warm catalyst operation, where mass transfer is the rate limiting step. Since the catalytic reaction only takes place in the walls of the catalyst, the pollutants in the exhaust gas have to diffuse to the wall, where they can undergo reaction. The state-of-the-art ceramic and metal catalysts that are in use today, utilize straight channels that run from one side of the catalyst to the other. Straight channel substrates have good mass transfer at the inlet of the channel, where the flow is still in a turbulent regime. However, the mass transfer rapidly drops as the flow becomes laminar along the channel. In laminar flow the highest concentration of pollutants is at the center of the channel, furthest from the wall. The pollutants have a long diffusion path to access the active reaction sites at the wall.

In the present work, innovative substrate technologies are presented that enable both a substrate mass reduction as well as an improvement in conversion efficiency by means of turbulent flow conditions in the single channel.

STRUCTURED CATALYST TUBES – WEIGHT REDUCTION THROUGH ENHANCED STABILITY

In addition to the matrix as substrate for the catalytically active coating the outer tube also offers potential for weight reduction by decrease of the wall thickness. However, tubes with small wall thicknesses have a proportionately smaller bending stiffness and inherent stability, which might be a disadvantage during production, canning and in service.

By forming three-dimensional vault-structures on the tube the stiffness can be improved considerably. Vault-structuring is a forming technique, with which three-dimensional structures are brought into thin-walled materials. Here either square or hexagonal shapes are possible. Multidimensional stiffening arise, through which the material develops higher bending and bulge stiffness. This technique allows tube material saving hence weight reduction while maintaining mechanical functionality of the component. Analog to naturally occurring structured materials, vault structuredTM (*) materials offer high stiffness at low wall thickness and low weight.

The production process of a cylindrical tube with vault structuring is based on tight-fitting, rigid support rings form the inside diameter, with a simultaneous pressure action on the outer side of the tube. After overcoming of a point of instability, square curving structures form spontaneously. Circumferential straight folds arise along with staggered folds in axial direction creating a uniform honey-comb structure. Subsequently the thin-wall material is considerably strengthened in all directions.

Vault structuring also has other advantages: Conventional structuring like rolling or punching takes place by flat contact to the forming tool and large force transmission. Local reductions in material thickness and diminished surface quality can be the result. In contrast, the vault structuring distinguishes itself from the conventional sheet-metal forming processes by an energy optimized self-organization process. Material, energy and resources are preserved, and the surface quality of the semi-finished product is retained.

*vault- structuredTM: Method Dr. Mirtsch GmbH; www.woelbstruktur.de Vault structured materials and processes are products of Dr. Mirtsch GmbH and protected by numerous national and international rights.

FEA STRESS SIMULATION

Through FEA computation the rigidities of a Standard mantel tube without structuring and a vault structured mantel tube are compared. Both mantel tubes have a wall thickness of 0.5 mm. In the simulation the mantel tubes are virtually positioned between two plates. Figure 1 shows the meshed Vault Structured Tube used for the simulation.



Figure 1: Meshed Vault Structured Tube

One of the plates is driven by 1 mm toward the second plate and the reaction force is evaluated (Figure 2). The computed reaction force is 14.4 N for the Standard tube without structuring, for the vault structured tube it is 23.7 N (Figure 3). The inherent stability is increased by 65% in this example under retention of the same wall thickness and therefore mass.

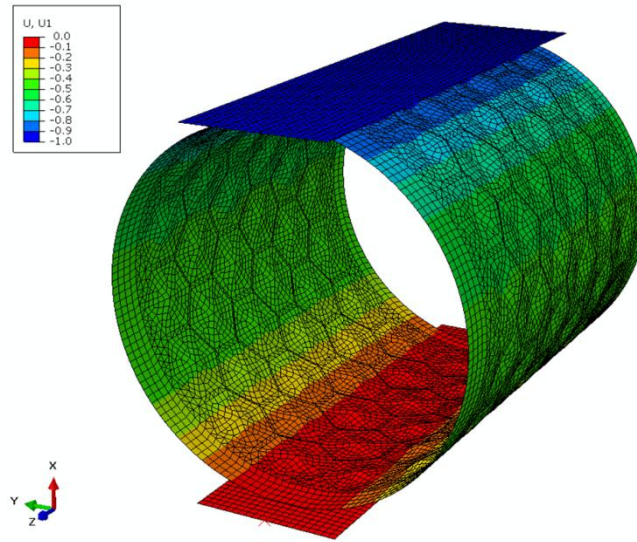


Figure 2: Simulation Model

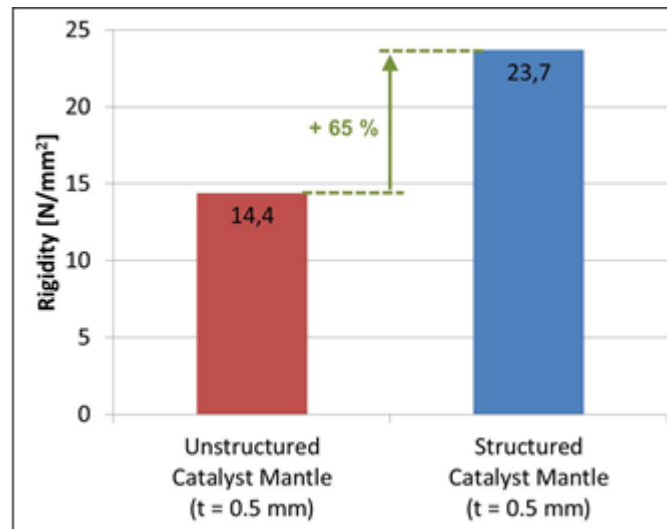


Figure 3: FEA Stress Simulation and Restoring Force

REDUCTION IN WEIGHT OF CATALYST

By this increase of the rigidity it is now in many cases practicable to reduce the wall thickness to 0.5 mm, where this was not possible before due to the low stiffness of the Standard tube. The component weight can be reduced by approx 30 % in case of a typical passenger car size substrate.

MECHANICAL ROBUSTNESS EXPERIMENTAL VALIDATION

In order to validate the design of the above described thin mantle an accelerated test procedure has been employed with superimposed thermal and mechanical loads. Both test equipment and durability results will be discussed in the next chapter.

TEST EQUIPMENT

Exhaust gas source

To simulate the thermal loads in an accelerated life test representative of real world conditions a burner system with an independent control of exhaust gas mass flow and exhaust gas temperature has been used. It is able to provide rapid gas temperature transients of +15000 K/min and -8000 K/min and an exhaust gas mass flow change rate (dynamics) of +/- 200 kg/h per second can be achieved.

Vibration source

The vibration of a vehicle application is typically a multi-axis load. To account for this effect, a two-axis excitation was required for the bench test. This was achieved by mounting the converter in an angle of 45° to the shaker vibration axis. The vector of force introduction is divided into two directions: axial (X) and radial (Y). For vibration control, accelerometers on water-cooled adaptors were used, which are directly mounted by welding to the converter mantle.

To ensure an introduction of vibration loads of 500 Hz and beyond to the test converter, a very rigid and stiff fixture was developed which allows frequencies up to 3000 Hz. The schematic principle of the vibration introduction into the test converter and the accelerometer setup is shown in Figure 15.

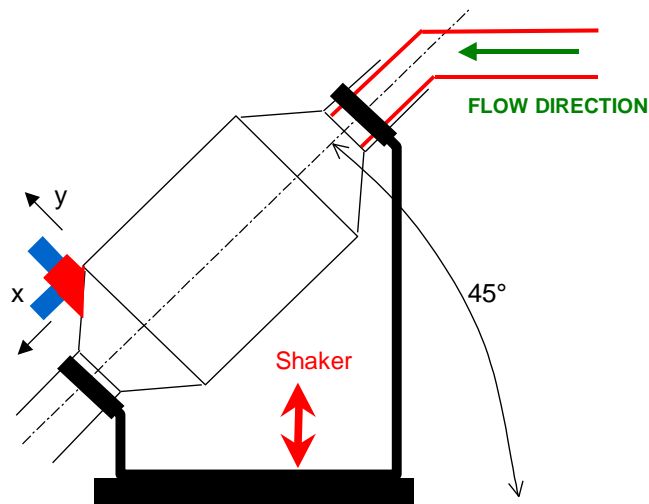


Figure 4 - Schematic principle for load introduction.

TEST RESULTS

Two substrates with 90x74.5mm matrix dimensions have been tested: one was equipped Standard converter mantle with 1.5mm wall thickness, the other featuring the innovative light-weight 0.5mm mantle with Vault structures.

A mass flow of 150 kg/h to 350 kg/h along with a temperature cycling of 830 °C to 330 °C has been applied, leading to a positive +5500 K/min and negative -2500 K/min temperature transients. Simultaneously a vibrational load of 10g RMS has been vertically put onto 45° fixture as sketched in Figure 4.

Based on an array of previous experiences and application programs, a lifetime of 50 hrs with no mechanical failure can be considered as a reference value.

As the 1.5mm thick mantle represents an industry Standard for the substrate dimensions mentioned above the test has been stopped at 66 hrs as no failure has taken place. Afterwards, the substrate with the 0.5 thin mantle with Vault structures has been tested according to the same thermo-mechanical loads. After 100hrs the test has been stopped as no evidence of failure could be reported here, proving the very good mechanical robustness of the innovative light-weight mantle and its feasibility for a real-life vehicular application. Photographic images of the gas inlet faces of both converters are shown in Figure 5 and Figure 6.



Figure 5 – Gas inlet face of the substrate with 1.5mm Standard mantle at 66hrs of the accelerated thermo-mechanical test.



Figure 6 – Gas inlet face of the substrate with 0.5mm Vault-structured mantle at 100hrs of the accelerated thermo-mechanical test.

TURBULENT FLOW MATRIX ARCHITECTURE

Laminar flow conditions occur behind the first section of the catalytic channel where the flow is not fully developed. Under laminar flow conditions the catalytic process is governed by the mass transfer (Figure 7).

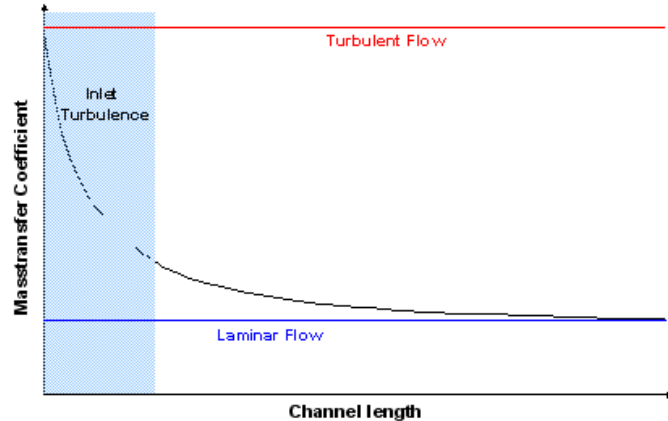


Figure 7: Mass transfer coefficient along the channel length

The figure shows how the mass transfer coefficient asymptotically approaches a low value just behind the inlet zone length. One way of increasing efficiency is the creation of turbulent flow conditions (Figure 8).

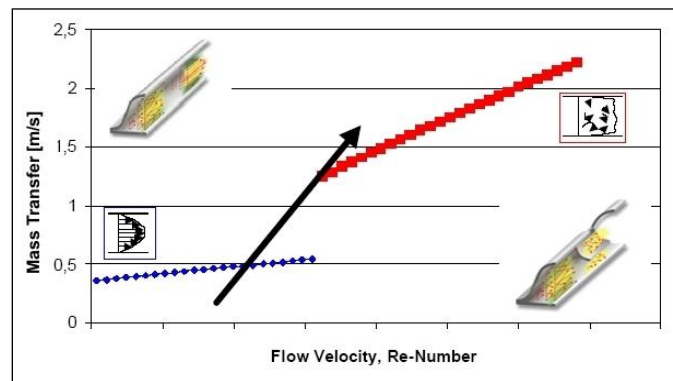


Figure 8 :Qualitative increase of the mass transfer coefficient from laminar to turbulent.

A fully turbulent flow in the catalytic converter would result in very high pressure drop. For this reason Emitec developed Perforated Foil (PE) and Longitudinal Structure (LS) substrates in which turbulence is generated locally. This approach not only increases the overall conversion efficiency but can also have a positive effect on pressure drop in PE and LS catalysts.

PERFORATED FOIL TECHNOLOGY

Perforated foil technology has already been successfully applied in the mass production of components for a variety of applications and has been discussed in detail in previous papers [1, 2]. PE technology (Figure 9) uses perforated flat and corrugated foils to generate radial flow between adjacent channels. The loss of GSA (geometrical surface area) is more than compensated by the generation of locally turbulent flow. The development of perforated metal foils offers many advantages:

- homogeneous distribution of flow and pollutant concentrations

- reduction of heat capacity
- reduction of pressure drop

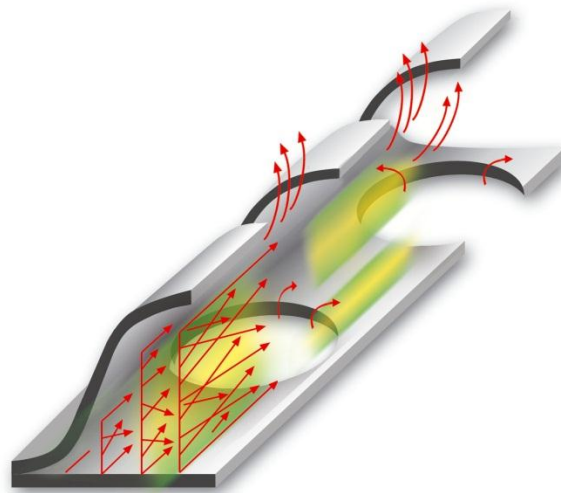


Figure 9: PE structure with flow details

In contrast to Standard catalysts, PE catalysts generate cross-flow, which gradually equalizes an inhomogeneous inlet flow. This exclusively turbulent compensating flow is driven by the radial pressure difference in the catalyst [3]. The result of this particular flow field backpressure in a PE catalyst is explained in Figure 10.

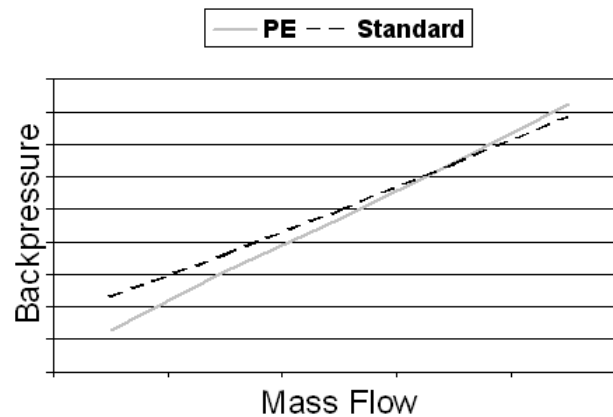


Figure 10: Qualitative backpressure representation of PE and Standard catalysts.

Figure 10 shows how the two lines representing the backpressure of Standard and PE catalysts intersect at a certain value of mass flow. The figure is only qualitative because the intersection point depends on many parameters such as washcoat loading and distribution, cell density and foil thickness. Tests carried out on an uncoated substrate showed that in this case the lines intersect at channel Reynolds (Re) numbers between 1500 and 1900. At low Re numbers the PE substrate has always lower backpressure than Standard substrates because the lower GSA and better internal flow distribution compensates the increase of backpressure given by the locally turbulent flow conditions. At high Re numbers the backpressure increase due to turbulent like condition is no more compensated and the total backpressure of a PE catalyst is higher than Standard substrate. Typical Re numbers in catalyst channels have values for which PE catalyst has a lower backpressure than Standard substrate.

LONGITUDINAL STRUCTURE TECHNOLOGY

The metallic longitudinal structure (LS) foil technology has been already extensively described and implemented in mass production [1]. The LS technology consists of a counter corrugation applied on the sinoidal part of the single channel in order to create some turbulent like areas.

In an LS channel (Figure 11) in correspondence of the counter corrugation, i.e. the shovel, the laminar flow is broken and a new “turbulent like” zone is created: thereby the efficiency of the catalytic converter is enhanced.

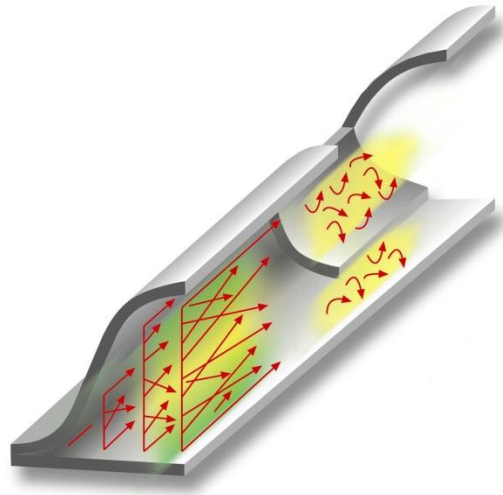


Figure 11: LS structure with flow details

It has already been demonstrated [4], how a metallic substrate with lower cell density but using LS technology can achieve the same conversion efficiency of a Standard converter with higher cell density.

ANALYTICAL EFFICIENCY INVESTIGATION

It is a well-known fact that catalyst effectiveness in warmed-up condition is influenced by substrate properties, i.e. by increasing the specific surface and improving contact between gas and wall, regardless of the type of catalytic reaction that is to take place. The key parameter that describes the transport properties is the mass transfer coefficient β , which is the analogue of the heat transfer coefficient α . Under mass transfer limited conditions catalyst effectiveness is linked to the coefficient β on the basis of the following correlation (formula 1):

$$\text{Formula (1): } U = 1 - \frac{c_{inlet}}{c_{outlet}} = 1 - \exp \left[- \frac{\beta GSA}{\dot{V}} \right]$$

The coefficient β can be expressed according to

$$\text{Formula (2): } \beta = \frac{Sh D_{12}}{d_h}$$

as a function of the Sherwood number, which itself depends primarily on key catalyst parameters, such as substrate length, hydraulic channel diameter and key flow parameters, such as the Reynolds number and the Schmidt number:

$$\text{Formula (3): } Sh = f(\text{Re}, Sc, d_h, L_{Cat})$$

The mass transfer coefficient describing the flux from the gas to the channel wall is known to depend very much on the shape and fluid dynamic design of the channel (i.e. the channel or catalyst structure). Typical options for the design of the channel shape include the introduction of secondary corrugations (LS structure) [5, 7] or holes in the channel wall [6].

It is of central importance that these structures are able to increase the value of the emission-relevant coefficient $\beta \times GSA$ under suitable operating conditions, as these values make it possible to design very compact substrates. Some of these structures also generate low backpressure, which in conjunction with high catalytic efficiency enables them to make an excellent contribution to solving the problems described in the introduction.

The above-mentioned computer models were defined on the basis of the following processes:

- Measuring the conversion rate under variation of design and process parameters and evaluation of the characteristic Sherwood numbers for Standard, PE and LS structures and for a ceramic substrate using propene oxidation on the gas test bench. Propene oxidation was chosen because mass transfer controlled regime begins here at fairly low temperatures (>350°C).
- From this basis correlations for Sherwood number as a function of Re , d_h and L was derived, as were the pressure loss models for each of the four structures by matching the measured data to typical equations that included all the above-mentioned parameters.
- In a next step, these equations were used to demonstrate the potentials of the individual structures with respect to the ratio between effectiveness and pressure loss on a comparative basis to select particularly advantageous structures.

EVALUATION OF CHARACTERISTIC SHERWOOD NUMBERS FOR VARIOUS SUBSTRATE STRUCTURES

In order to obtain reproducible results the tests were carried out on a gas test bench because the boundary conditions (mass flow, temperature and thermal management) could be kept easily at a constant level. Figure 12 shows a sketch of the reactor used in the test.

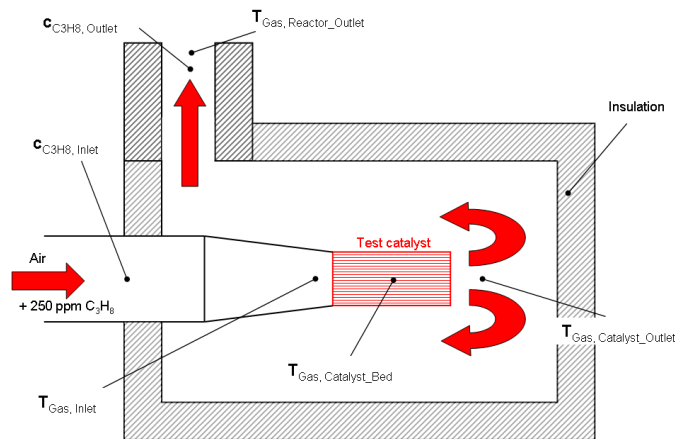


Figure 12: Diagram of the test reactor used to determine the mass transfer coefficient during propene oxidation

The test bench was operated under almost isothermal conditions, which were achieved by a low propene concentration (250 ppm) and optimised gas flow guidance. The following catalysts were tested, all catalysts have a diameter of 40mm, a coating mass of 110 [g/l] except the PE that has 88 [g/l] and 50 [g/ft³] Pt only coating.:

Length [mm]	Cell density [cpsi]	Structure
50.8	200	Standard
20	600	Standard
50.8	200 / 400	LS
50.8	200	PE
50.8	200	Ceramic

Table 1: Overview of catalyst data to determine the mass transfer coefficients during propene oxidation.

The catalysts listed in the table were measured not just at a single length but also at lengths ranging from 5 to 50.8 mm. The lengths were $L = 11.9 / 15.9 / 22.9 / 26.9 / 35.9 / 38.9 / 47.9 / 50.8$ mm in case of 200 cpsi or $5 / 8 / 11 / 14 / 17 / 20$ mm in case of 600 cpsi. Tests had to be performed at sufficiently high temperatures to ensure mass transfer limitation. Since the objective was a correlation between Sh and Re , L and d_h the following values were varied within defined limits:

- Temperature 100 – 600 °C in 50 K steps. Only test results obtained well above 300°C have been taken into consideration for evaluation of mass transfer coefficients
- Mass flow 5 – 50 kg/h
- Cell density: 200 – 600 cpsi
- Catalyst length: 5- 50.8 mm

This produced a large pool of data for the following fit parameters that are relevant to the adaptations of the Sh correlation according to formula (3):

- Reynolds number Re (\Rightarrow mass flow, temperature, hydraulic diameter)
- Hydraulic diameter d_h (\Rightarrow cell density)
- Catalyst length
- Schmidt number Sc (\Rightarrow temperature, gas species)

The tests were conducted in the form of light-off curves at constant catalyst length, cell density and mass flow at temperatures ranging from 100 to 600 °C in 50 K steps. The resulting data were filtered for mass transfer limitation and the relevant data sets were used to generate the mass transfer coefficient according to formula 1 and from this the Sh numbers, for which a fit was carried out in a final step.

Figure 13 shows the results in the form of Sh as a function of Re for three substrate types with different structures as measurement results. The LS structure can be seen to have great advantages conceptually over the smooth Standard channel, while the PE structure produces higher Sh numbers than the Standard channel. This fact is easily explained by the additional number of edges in substrates with an LS or PE structure where the flow boundary layer has to be re-established in terms of inlet flow [8, 9, 10].

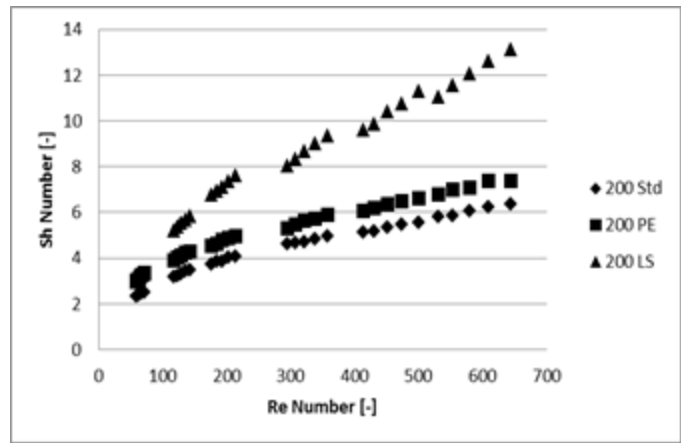


Figure 13: Plot of Sh curves over Re for three different catalyst structures at temperatures ranging from 300 to 600°C

The data were then fitted to obtain a correlation for Sherwood in the form of $Sh = f(Re, d_h, L_{catalyst}, Sc)$. This resulted in the following correlation:

$$\text{Formula (4): } Sh = Sh_{lim1} + A \left(\frac{Re}{B} \right)^C \frac{DGz^E}{1 + FGz^G}$$

with Sh_{lim} , A, B, C, D, E and as dimensionless parameters different for each type of structure and Gz being Graetz number.

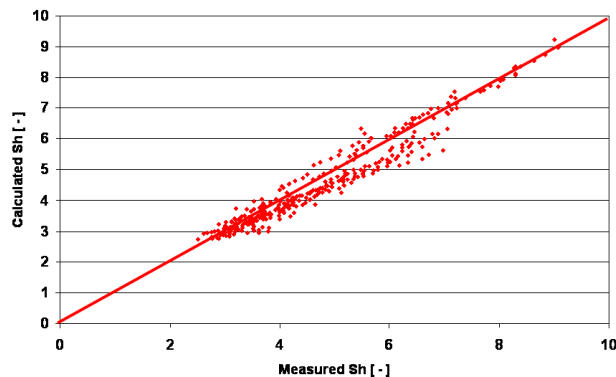


Figure 14: Comparison between measured and calculated Sherwood numbers for the Standard structure (metal)

Figure 14 displays the result of the fit for the Standard structure as an example. The graph reveals a satisfying agreement between measurement and correlation ($R = 0,954$).

CALCULATION OF CATALYST PERFORMANCE PARAMETERS FOR VARIOUS METAL SUBSTRATE STRUCTURES

On the basis of the correlations derived in the previous section it was now possible to determine parameters for all catalysts to describe their catalytic effectiveness at operating temperatures and the amount of pressure loss and to compare the structures to each other.

The comparison has been done on substrates listed on

Table 2. All catalysts have been regarded on the basis of the same dimensions (Ø40mm, length 50.8mm) and same amount of coating (140 g/l) under the variation of exhaust mass flow at a constant temperature of 450°C.

Figure 15 shows the calculated $\beta \times \text{GSA}$ values for metal and ceramic substrates with four basic cell densities of 200, 300, 400 and 600 cpsi as a function of channel velocity at 450°C.

Cell density [cpsi]	Wall thickness [μm / mil]	Structure
400	50	Standard
600	50	Standard
200 / 400	50	LS
300 / 600	50	LS
400	50	PE
600	50	PE
400	4,5	Ceramic
600	3,5	Ceramic

Table 2: Overview of catalyst data used to calculate $\beta \times \text{GSA}$ values, pressure loss and CPC coefficients

The following phenomena can be derived from the data:

- Both LS structures are substantially more affected by channel velocity than any other type
- This means that there is a typical channel velocity for each type of substrate above which it can be replaced by an LS structure with lower basic cell density (for example: LS 200/400 replaces 400 Standard Metallic at a velocity above approx. 10 m/s)
- On the other hand, PE structures behave similarly to Standard channels, although compared to the Standard (Metallic and Ceramic) substrates the $\beta \times \text{GSA}$ value for PE is not reduced to the extent expected due to the GSA loss. This results from a gain in β of PE relative to the Standard structure
- The values for (Standard) metal and ceramic structures are almost identical at comparable cell densities.

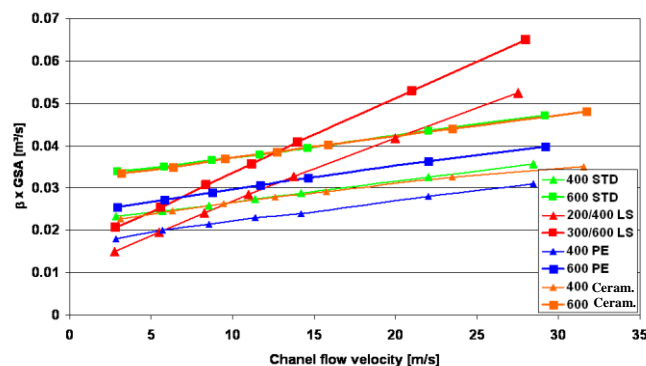


Figure 15: Calculated values of $\beta \times GSA$ at 450°C for different substrate structures as a function of channel velocity (140 g/l washcoat)

In addition, the calculated pressure losses for the same structures are plotted in Figure 16.

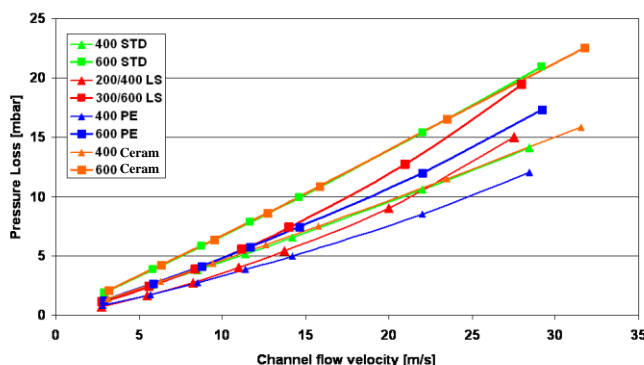


Figure 16: Calculated backpressure values at 450°C for different substrate structures as a function of channel velocity (140 g/l washcoat)

The following can be observed:

- At flow speeds not exceeding 15-20 m/s both LS structures produce significantly less backpressure than substrates whose basic cell density is twice as high (for example: 15 m/s; LS 300/600 approx. 7.5 mbar, 600 Standard Metallic approx. 10 mbar)
- At higher flow speeds the backpressure in LS structures rises to levels that correspond to those of substrates whose basic cell density is twice as high (for example: 30 m/s; LS 300/600 approx. 30 mbar, 600 Standard Metallic approx. 30 mbar)
- On the other hand, PE structures have a significant pressure loss advantage over a wide speed range in this respect compared to Standard substrates with an identical cell density [4, 6]. This advantage is slightly reduced at very high flow speeds.
- The values for Standard metal and ceramic substrates are very similar at same channel velocity. Actually, as backpressure goes with mas flow, ceramic substrates would show greater backpressure due to higher channel velocity (thicker walls, smaller porosity) at same mass flow.

As defined in previous publications, “practical” catalyst performance for structured substrates relative to smooth-channel types is characterised by the potential for improving $\beta \times GSA$ in relation to an increase in backpressure (each again in relation to the values of the smooth-channel substrate). This has already been described in earlier papers on the basis of the CPC (catalyst performance factor) [11].

$$\text{Formula (5): } CPC_{Structure} = \frac{(\beta \cdot GSA)_{Structure}}{(\beta \cdot GSA)_{Standard}} = \frac{\Delta p_{Structure}}{\Delta p_{Standard}}$$

In Figure 17 the CPC of the structures described above is plotted versus the 400 cpsi STD (metal). The data shown are derived from the previous two plots.

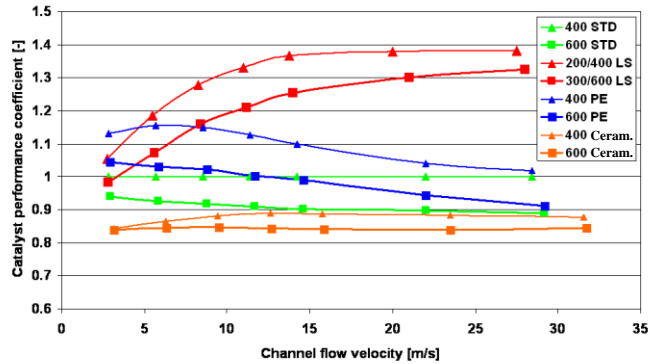


Figure 17: Calculated CPC values [11] at 450°C for different substrate structures as a function of channel velocity (140 g/l washcoat)

In summary the following can be said about the CPC:

- Maximum values for CPC, that is, the best ratio between effectiveness and backpressure, is apparently achieved by the LS structure. This is made possible by a high β value at fairly low backpressure. Due to even lower backpressure smaller cell density offers particular advantages, whereas high conversion rates are more easily achieved by the application of higher cell density.
- The results for PE substrates are between those of LS designs and Standard substrates depending on flow speed. The surface loss can be partially offset by a higher β , while significantly lower backpressure provides the main potential.
- At a similar β as the STD metal substrates but lower GSA and higher backpressure the two ceramic substrates tend to show lower CPC.

These observations clearly show that the application of an LS design, particularly with a cell density of 300/600 cpsi, offers advantages when used at warm operating temperature and at sufficiently high flow speeds or when there is the needs of a very compact catalytical converter.

On the other hand, PE substrates show a clear advantage in Backpressure and can compensate the loss of GSA having higher value of β than Standard substrate.

EMISSION MEASUREMENTS: LS DESIGN VS. STD CHANNEL

EXPERIMENTAL SETUP

An experimental back-to-back comparison between Standard metallic substrate and turbulent-like LS-Design substrate has been carried out on an automotive spark ignition engine. The powertrain unit used for this testing is a 6 cylinder with 3,4 Liter displacement and a rated power of 217 kW installed on a chassis dyno test bench.

Two different TWC catalytic converter layouts have been chosen to carry out the comparison. On one hand a Standard metallic substrate Dia 115x80mm (V= 0,831 liter) with 400cpsi cell density and on the other turbulent-like substrate with same dimensions and 300-600LS cpsi. Both substrate are round with Dia 115x80 mm matrix dimensions, 0,831 Liter volume and 40 μ m foil thickness.

It can be seen from

Table that the GSA of the 300-600LS substrate is 15% lower compared with the 400 Standard metallic substrate due to the lower main cell density employed in the LS converter. The difference in cell density, i.e. foil material used in the substrate, leads to another

important difference: the thermal capacity, which is about 14% lower compared with that of the reference 400 Standard metallic substrate.

Substrate design	GSA [m ²]	Cp [J/K]
115x80/400/40	2.8	223
115x80/300-600LS/40	2.4	193

Table 4 – Main characteristics of tested substrates

The metal substrates have been coated with 90 gr/ft³ at 0/14/1 weight ratio.

The substrates have been hydrothermally aged for 4 h @ 980 °C before emission testing.

On each exhaust system layout, 5 repetitions of the NEDC test cycle have been carried out, where the first one has been used only as preconditioning. Raw emission as well as tailpipe emissions downstream the catalyst have been modally recorded. CVS bag values have been sampled as well.

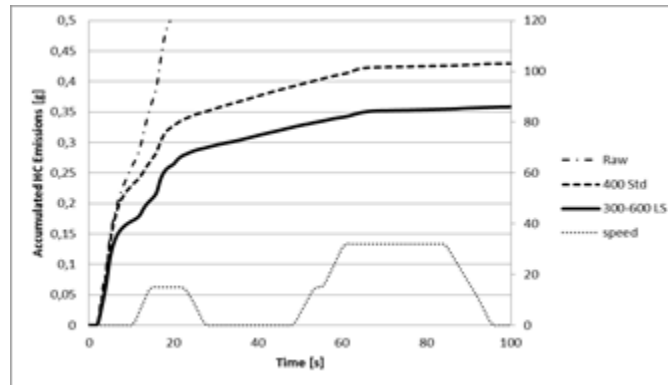
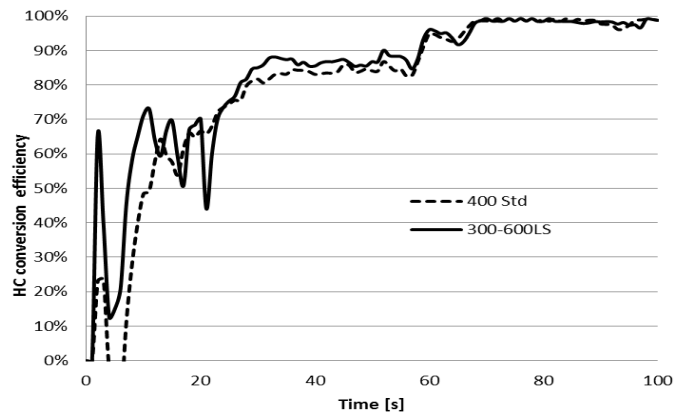


Figure 18 Comparison of accumulated HC tailpipe emissions of 400 Standard metallic and 300-600LS substrate during cold start phase of NEDC Test Cycle

In Figure 18 accumulated HC tailpipe emissions are reported for the first 100 sec of the NEDC cycle. It can be clearly noticed that the LS substrate starts its conversion activity at 8 seconds after engine cranking while the 400 Standard metallic converter starts its



catalytic activity approximately 4 seconds later (see also [Page 15 of 19](#))

Figure 19). Consequently, at sec. 10, the LS converter shows already 23% lower tailpipe emissions. The higher performance of the 300-600LS converter is due to its 14% lower thermal capacity compared with the 400 Standard metallic matrix, which plays an important role in the first seconds of the NEDC where it is crucial to transfer the exhaust gas heat energy to the catalyst bed as quick as possible, also in order to minimize the CO₂ penalty related to engine-based cat heating strategies (Figure 20).

It has to be noticed also, that the LS-Structure enables a 14% substrate mass reduction compared to the Standard 400 cpsi substrate.

An additional advantage accumulation of the turbulent-like converter can be observed in the time window between sec 20 and 50 where the second hill of the ECE part is reached. During this phase, it can be observed in

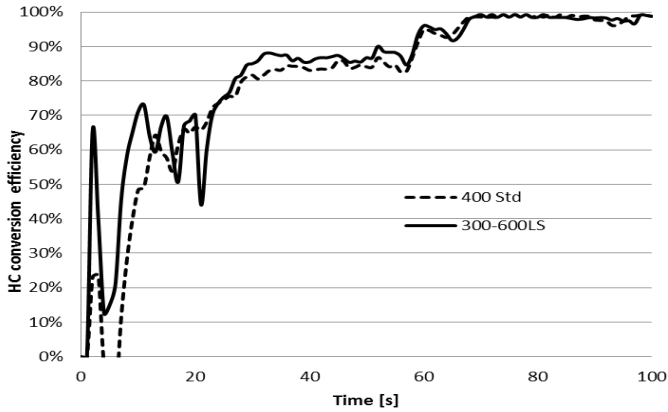


Figure 19 how the conversion efficiency of the LS substrate, although not yet fully developed at 100 %, is approx. 5% higher than that of the converter using 400 cpsi Standard technology.

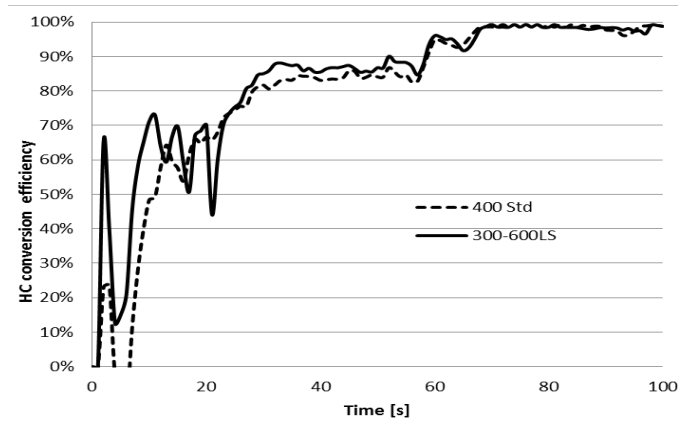


Figure 19 HC Conversion Efficiency during the first 100 sec. of the NEDC

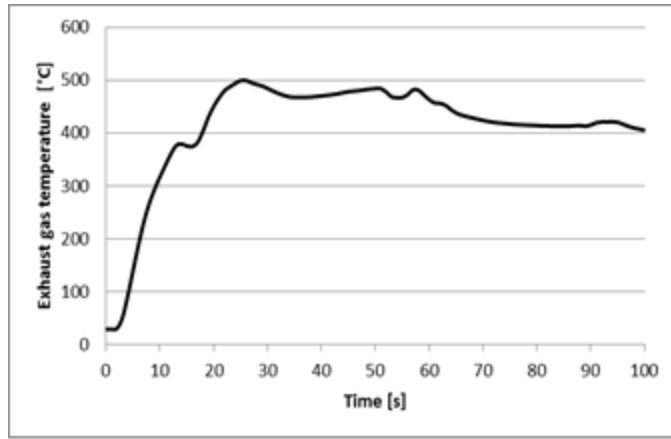


Figure 20 Exhaust gas temperature in front of catalyst during the first 100s of the NEDC

The remaining part of the 1st ECE module does not show further changes in emission profile, as the 2 curves evolve almost in parallel fashion, yielding 16% lower tailpipe emissions of the 300-600 LS substrate compared to the result of the 400 cpsi Standard converter at sec 100.

In order to better analyze the hot phase emissions, the tailpipe figures have been separated from the ECE modules resetting the bag value at 0 g.

In Figure 21 accumulated HC tailpipe emissions along only the EUDC module of the NEDC Test Cycle are reported. It can be clearly noticed that even if the LS substrate has 15% lower GSA with respect to the 400 Standard metallic converter, it remarkably outperforms the 400Standard metallic converter starting at the 1st plateau of the EUDC. This higher efficiency leads to 33% lower tailpipe emission with respect to the EUDC bag.

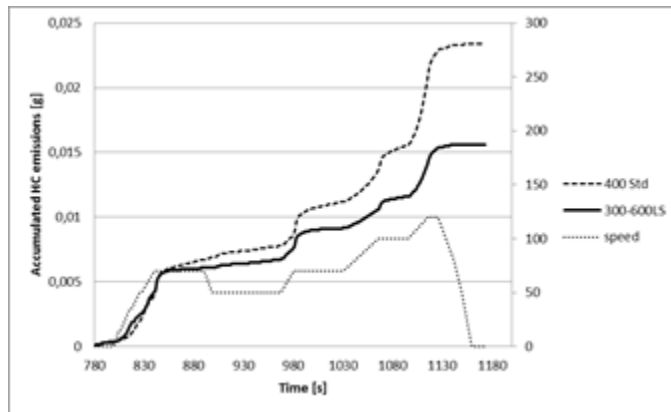


Figure 21 – Comparison of accumulated HC tailpipe emissions of 400 Standard metallic and 300-600LS substrate during the EUDC module of the NEDC Test Cycle

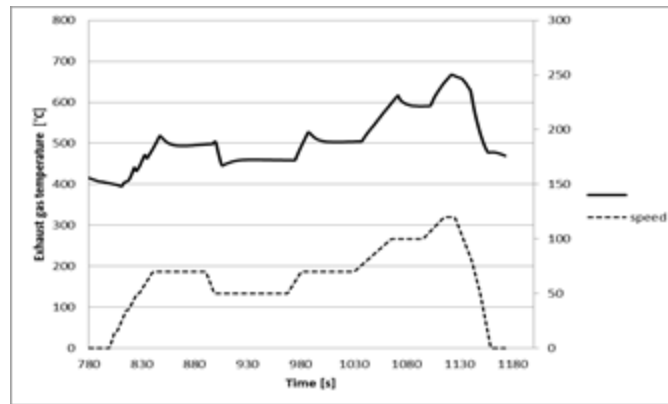


Figure 22 – Exhaust gas temperature in front of catalyst during the EUDC module of the NEDC

It can be noticed from Figure 22 that the exhaust gas temperature in front of the catalyst during the EUDC module of the NEDC is well above the typical light-off window of a classical 3-way catalytic coating. Hence it can be stated that in this phase the conversion reaction is mass transfer limited and the heat capacity properties of the different substrate designs do not influence the overall performance anymore. The micro-scale turbulence created in the channels of the structured LS substrate yields to a higher mass transfer coefficient. As a result, better conversion efficiency in the warm phase of the NEDC cycle is achieved.

SUMMARY/CONCLUSIONS

An innovative substrate mantle design with thin wall structured construction and light weight characteristic has been investigated by means of FEM simulation. It has been highlighted how the Vault-structure design of the mantle allows to reduce wall thickness from 1.5mm to 0.5mm leading to approximately 30% converter weight reduction. The FEM analysis has shown how the Vault-structures of the mantle yield a rigidity increase of about 65% compared to a 0.5mm thick mantle with no structures on it. The light weight mantle design has been durability proven by means of an accelerated key-life test performed on a hot shaker with superimposed thermo-mechanical loads. A direct comparison between the 0.5mm Vault-structured and the Standard 1.5mm mantle showed that the durability targets have been fully achieved.

The present paper deals also with the improvement of flow characteristics inside the substrate by means of turbulent-like foil structures leading to enhanced mass transfer properties, represented by the Sherwood number.

At first an experimental investigation comparing Standard substrates with LS- and PE-substrate focusing on the Sherwood number has yielded a superiority of LS-design at higher Re-number. Secondly a numerical correlation has been identified to calculate Sh Numbers of different catalyst designs as a function of channel Re-number. The results presented show that the LS structure produce significantly less backpressure than substrates whose basic cell density is twice as high.

For practical experience it has been shown in previous works that the CPC parameter (Catalyst Performance Coefficient) is more meaningful to draw conclusions about expected catalyst efficiency both from an emission conversion perspective as well as from a backpressure standpoint. Comparisons of different cell structures based on the CPC coefficient highlight the potential of the LS structure to achieve high emission performance while keeping limited backpressure impact on the exhaust gas system.

Based on these expectations, an experimental emission measurement has been carried out on a chassis dyno in order to compare Standard cell structure (laminar flow) with an LS-design converter. Both cold-start and warm-operation emissions have been recorded. The results show a superiority of the LS-Design during the cold start, which is related to the reduced thermal mass of the LS (in comparison with the reference Standard design). A separated bag sampling during the EUDC part of the NEDC cycle has highlighted the superior performance of the LS also during this phase, where overall conversion efficiency is not influenced by thermal mass rather by mass transfer properties, which are improved in the LS design due to local micro-turbulence taking place at the secondary corrugation of the channel.

Additionally, the LS design tested in the present work, enables 14% substrate mass reduction compared to the Standard catalytic converter in the same test.

As a conclusion, both outer mantle design and inner substrate architecture can be successfully designed in a metal support catalyst in order to meet future emission legislation while limiting to a minimum the backpressure and weight impact in view of the increasingly demanding CO2 targets.

REFERENCES

1. M. Bollig, J. Liebl, R. Zimmer BMW Group, M. Kraum, O. Seel, S. Siemund, Engelhard Technologies GmbH, R. Brück, J. Diringer, W. Maus, Emitec GmbH: “Next generation catalysts are turbulent: development of support and coating”, SAE-Paper 2004-01-1488,
2. M. Ganz, S. Hackmayer, quattro GmbH, C. Kruse, A. Reck, Emitec GmbH “Innovatives Katalysatorsystem für den Audi RS6, 8 Zyl, 4,2ltr, 331 KW mit LEV Zertifizierung”, Wiener Motoren Symposium, 29-30. April 2004
3. Dr. Rolf Kaiser, Florian Stadler - ArvinMeritor Emissions Technologies GmbH Lorenzo Pace, Dr. Manuel Presti – Emitec GmbH: “Simulationsmodell von Drei-Wege-Katalysatoren mit perforierten Folien”, MTZ 05.2007
4. Lorenzo Pace, Roman Konieczny, Manuel Presti, Emitec GmbH, “Metal Supported Particulate Matter-Cat, a Low Impact and Cost Effective Solution for the FIAT 1.3 JTD Euro IV Engine”, SAE Paper 2005-01-0471
5. W. Maus, R. Brück; Emitec GmbH; “Die Zukunft der heterogenen Katalyse im Automobil; Turbulente Katalysatoren für Otto- und Dieselanwendungen”; 26. Internationales Motorensymposium, Wien, 27.04.2005
6. C. Iotti, V. Rossi, L. Poggio; Ferrari S.p.A.; M. Holzinger; ArvinMeritor; L. Pace, M. Presti; Emitec GmbH; “Backpressure Optimized Close Coupled PE-Catalyst - First Application on a Maserati Powertrain”; SAE-Paper 2005-01-1105
7. Deutschmann, N. Mladenov; TU Karlsruhe; W. Maus, R. Brück, P. Hirth; Emitec GmbH; “Turbulent schlägt laminar ”; 27. Internationales Motorensymposium, Wien, 2006
8. W. Bohl; “Technische Strömungslehre”; Vogel-Verlag
9. VDI-Wärmeatlas
10. H.-D. Baehr, K. Stephan; “Wärme- und Stoffübertragung”; Springer-Verlag
11. J. Liebl; BMW Group; W. Maus, R. Brück; Emitec GmbH; “Strengere Abgas-Emissionsgesetze - Niedrigste CO2- und Schadstoff-Emissionen,ein lösbarer Zielkonflikt?”; ATZ / MTZ-Konferenz – Energie; München; 2006

CONTACT INFORMATION

DEFINITIONS/ABBREVIATIONS

C_{inlet}	Inlet concentration
C_{outlet}	Outlet concentration
GSA	Geometric Surface Area
\dot{V}	Volumetric flow
D_{12}	Diffusivity
d_h	Hydraulic diameter
L_{kat}	Substrate length
Sc	Schmidt number